

A Monte-Carlo Approach to Zero Energy Quantum Scattering*

Stefan Lenz

*Center for Theoretical Physics, Sloane Physics Laboratory,
Yale University, New Haven, CT 06520-8120, USA*

Hubertus Mall

*Institut für theoretische Physik 3, Universität Erlangen,
Staudtstr. 7, 91058 Erlangen, Germany*

Abstract

Monte-Carlo methods for zero energy quantum scattering are developed. Starting from path integral representations for scattering observables, we present results of numerical calculations for potential scattering and scattering off a schematic ${}^4\text{He}$ nucleus. The convergence properties of Monte-Carlo algorithms for scattering systems are analyzed using stochastic differential equation as a path sampling method.

*This work was supported in parts by the DFG Graduiertenkolleg 'Starke Wechselwirkung' Erlangen-Regensburg, by the Bundesministerium für Forschung und Technologie (BMFT) and the Department of Energy Grant DE-FG02-91ER40608 (S.L.).

I. INTRODUCTION

Quantum scattering problems play an important role in many branches of physics. Almost all our knowledge about composite microscopic systems is obtained from scattering experiments. The theoretical analysis of these experiments is particularly difficult if the target has internal degrees of freedom which couple strongly to the projectile. Examples of this situation are antiproton-nucleus and K^- -nucleus scattering. Since nucleon-antiproton or nucleon- K^- scattering length is of the same order of magnitude as the typical internucleon distance [1–3], one expects that nuclear scattering of these projectiles is dominated by multiple scattering correlations involving many nucleons.

The standard approach to low energy nuclear multiple scattering is the construction of effective optical one-body potentials [4]. It has been possible to describe successfully the phenomenology of elastic scattering and inelastic reactions to specific channels [1,2] as well as exotic atoms [5] in the framework of optical potentials.

One essential shortcoming of the optical model is that it is very restricted from the point of view of nuclear dynamics. Phenomenological difficulties in the description of the strong annihilation in antiproton-nucleus and K^- nucleus scattering are attributed to missing dynamical properties of simple optical potentials [6]. Recently it has been shown that a model which is dynamically richer than the optical potential is able to produce the observed large annihilation [7,8].

This example shows that the development of alternative methods for multiple scattering problems is necessary to understand important aspects of nuclear reactions. For many-body problems with a discrete spectrum considerable progress has been achieved by using Monte-Carlo techniques [9,10]. They have been applied to quantum field theories [11], atomic nuclei [12,13], quantum liquids [14–17] and other problems in condensed matter physics [18,19]. However, for scattering problems with a many-body system as target, standard Monte-Carlo methods are not applicable. The fact that scattering wave functions are not normalizable, and that the spectrum is continuous, requires the development of methods

which are specifically designed for scattering problems.

In this paper, methods are presented, which allow for the calculation of scattering observables at vanishing projectile energy. Their convergence behaviour is estimated using stochastic differential equations as a path sampling method. A schematic many-body problem is discussed in order to demonstrate that the methods developed for potential scattering are applicable to more complicated systems.

This paper is organized as follows: In section II three different path integral representations of scattering observables at zero energy are derived. In section III numerical algorithms are developed from these path integral representations and applied to scattering off a Gaussian potential. The convergence properties for scattering problems are compared with systems which possess a bound state. In section IV scattering off a schematic ${}^4\text{He}$ nucleus is treated. A discussion of the results is given in V.

II. SCATTERING OBSERVABLES AND THE PATH INTEGRAL

A. Path integrals

In this section we briefly review the path integral formalism following the presentation in [20]. The Monte-Carlo methods developed in this paper are based on a path integral representation of the imaginary time propagator:

$$\rho(\vec{x}_f, \vec{x}_i|\beta) = \langle \vec{x}_f | \exp(-\beta H) | \vec{x}_i \rangle$$

For a Hamilton operator H which is the sum of kinetic energy and a local potential $V(x)$

$$H = H_0 + V(\vec{x}) = \frac{\vec{p}^2}{2m} + V(\vec{x})$$

one finds from the Trotter product formula [20]

$$\rho(\vec{x}_f, \vec{x}_i|\beta) = \lim_{N \rightarrow \infty} \prod_{j=1}^{N-1} \int d^3x_j \left(\frac{m}{2\pi\epsilon} \right)^{3/2} \exp(-S[x]) =: \int Dx \exp(-S[x]) \quad (1)$$

$$S[x] = S_0[x] + S_V[x] \quad S_0[x] = \sum_{n=0}^{N-1} \frac{m}{2\epsilon} (\vec{x}_{n+1} - \vec{x}_n)^2 \quad S_V[x] = \sum_{n=0}^{N-1} \epsilon V(\vec{x}_n), \quad (2)$$

with $\vec{x}_0 = \vec{x}_i$, $\vec{x}_N = \vec{x}_f$ and $\epsilon = \beta/N$.

Using the spectral decomposition of the propagator one sees that the ground state wave function can be extracted from it in the limit $\beta \rightarrow \infty$. For a system with a discrete spectrum one finds:

$$\rho(\vec{x}_f, \vec{x}_i|\beta) = \sum_{n=0}^{\infty} \psi_n(\vec{x}_f)\psi_n^\dagger(\vec{x}_i) \exp(-\beta E_n) \stackrel{\beta \rightarrow \infty}{\approx} \psi_0(\vec{x}_f)\psi_0^\dagger(\vec{x}_i) \exp(-\beta E_0) \quad (3)$$

ψ_n are energy eigenstates of the Hamilton operator H and E_n the corresponding eigenvalues. Therefore solving the high dimensional integral (1) yields information about the ground state of a physical system. Numerical algorithms for calculating the integral (1) can be formulated using importance sampling techniques [10]. The convergence rate in β in (3) is controlled by the energy gap between the ground state and the first excited state. Excited states decay exponentially. This is a typical property of systems with a discrete spectrum.

The spectrum of a scattering system in absence of a bound state is purely continuous, i.e. there is no energy gap. Like in the case of a discrete spectrum the imaginary time propagator can be written in terms of a complete set of eigenfunctions of the Hamiltonian [21]

$$\rho(\vec{x}_f, \vec{x}_i|\beta) = \int d^3k \langle \vec{x}_f | \psi_k^+ \rangle \langle \psi_k^+ | \vec{x}_i \rangle \exp(-\beta \frac{\vec{k}^2}{2m}) \stackrel{\beta \rightarrow \infty}{\approx} \left(\frac{2\pi m}{\beta} \right)^{3/2} \psi_{k=0}^\dagger(\vec{x}_i) \psi_{k=0}(\vec{x}_f). \quad (4)$$

The states $|\psi_k^+\rangle$ are scattering wave functions with projectile energy $E = \vec{k}^2/(2m)$. They are solutions of the Lippmann-Schwinger equation [22]:

$$|\psi_k^+\rangle = |\vec{k}\rangle + \frac{1}{E - H_0 + i\epsilon} V |\psi_k^+\rangle,$$

where $|\vec{k}\rangle$ is a momentum eigenstate. Alternatively we could have used solutions $|\psi_k^-\rangle$ with ingoing wave boundary conditions

$$|\psi_k^-\rangle = |\vec{k}\rangle + \frac{1}{E - H_0 - i\epsilon} V |\psi_k^-\rangle,$$

or an arbitrary linear combination of these functions in equation (4).

From equation (4) one sees that for systems with a continuous spectrum the ground state can also be found from the large β limit of the imaginary time propagator. In numerical calculations two closely related problems occur: The scattering wave functions are not normalizable and due to the lack of an energy gap excited states are only suppressed like $1/\beta$. Therefore long imaginary times are necessary. In a Monte-Carlo algorithm this causes large fluctuations which have to be suppressed by generating many path samples. In order to use Monte-Carlo methods for systems with a continuous spectrum it is particularly important to construct estimators for physical observables with a small variance in order to avoid long computation times. In the following sections we derive relations between the imaginary time propagator and scattering observables which can be used to find estimators for these observables.

B. The cross section at $E = 0$

In [21], equation (3) is used together with the asymptotic form of the wave function at $E = 0$

$$\psi_{k=0}^+(r) \stackrel{r \rightarrow \infty}{\cong} 1 + \frac{a}{r}; \quad \sigma(E = 0) = 4\pi a^2, \quad (5)$$

to derive a variational principle for the scattering length a and the cross section σ . For a numerical calculation of the scattering length with Monte-Carlo methods, the following relation between scattering length and scattering wave function [22] is more suitable as it does not require the limit $r \rightarrow \infty$:

$$a = -\frac{2m(2\pi)^3}{4\pi} \lim_{k \rightarrow 0} \langle \vec{k} | V | \psi_{k=0}^+ \rangle. \quad (6)$$

With this expression one can show that the cross section at $E = 0$ can be found from a matrix element of the imaginary time propagator

$$\sigma(E = 0) = \lim_{\beta \rightarrow \infty} (2\pi m \beta)^{1/2} 2\beta (2\pi)^3 \langle k = 0 | V e^{-\beta H} V | k = 0 \rangle. \quad (7)$$

This can be expressed as a path integral by using (1):

$$(2\pi)^3 \langle k=0 | V e^{-\beta H} V | k=0 \rangle = \int d^3 x_f d^3 x_i V(x_f) V(x_i) \int_{\vec{x}_{i,0}}^{\vec{x}_{f,0}} Dx \exp(-S[x])$$

This result is generalized to scattering off a target with internal degrees of freedom in section IV.

C. The phase shift

An alternative path integral representation of the scattering length can be found from the equation [21,23]

$$\Delta Z(\beta) = \text{Tr} e^{-\beta H} - \text{Tr} e^{-\beta H_0} = \sum_{l=0}^{\infty} \frac{2l+1}{\pi} \int_0^{\infty} dk \exp(-\beta \frac{k^2}{2m}) \frac{\partial \delta_l(k)}{\partial k}, \quad (8)$$

which relates the scattering phase shifts $\delta_l(k)$ of a system with its statistical properties. Like (3), this equation holds if there are no bound states of the projectile. Note that both traces in the equation (8) are infinite for a system with a purely continuous spectrum.

Using the Trotter product formula we find again a path integral representation for (8)

$$\begin{aligned} \Delta Z(\beta) &= \int Dx \exp(-S[x]) \\ S[x] &= S_0[x] - \ln(e^{-S_V[x]} - 1). \end{aligned} \quad (9)$$

The paths are periodic in β , i.e. $\vec{x}_N = \vec{x}_0$. Problems which are related to the logarithm in the exponent of (9) will be discussed later. In the limit $\beta \rightarrow \infty$ one finds from the threshold behaviour of the scattering phase shifts $\lim_{k \rightarrow 0} \delta_l(k) = a_l k^{2l+1}$ that ΔZ is proportional to the s-wave scattering length $a = a_0$

$$a = \lim_{\beta \rightarrow \infty} \pi \left(\frac{2\pi m}{\beta} \right)^{1/2} \Delta Z(\beta). \quad (10)$$

D. The scattering length and the virial theorem

An alternative method for calculating of the scattering length can be found from the scale transformation properties of the transition matrix T . The transition matrix is defined as

$$T(E)|\vec{k}\rangle = V|\psi_k^+\rangle. \quad (11)$$

One can show that [24]

$$\frac{d}{dp}p\langle\vec{p}_f|T(E)|\vec{p}_i\rangle = -\langle\psi_{p_f}^{(-)}|o(\vec{x})|\psi_{p_i}^{(+)}\rangle \quad (12)$$

$$p = |\vec{p}_f| = |\vec{p}_i| = \sqrt{2mE} \quad (13)$$

$$o(\vec{x}) = 2V(\vec{x}) + \vec{x} \cdot \vec{\nabla}V(\vec{x}). \quad (14)$$

A proof of this formula is given in appendix A.

With this equation one can derive a path integral relation for the scattering length a . First the spectral decomposition of the imaginary time propagator in terms of the scattering wave functions $|\psi_k^+\rangle$ and $|\psi_k^-\rangle$ is used:

$$\frac{\int d^3x \langle\vec{x}_f|\exp(-\frac{\beta}{2}H)|\vec{x}\rangle o(\vec{x}) \langle\vec{x}|\exp(-\frac{\beta}{2}H)|\vec{x}_i\rangle}{\langle\vec{x}_f|\exp(-\beta H)|\vec{x}_i\rangle} \stackrel{\beta \rightarrow \infty}{=} \left(\frac{16\pi m}{\beta}\right)^{3/2} \langle\psi_{k=0}^-|o(\vec{x})|\psi_{k=0}^+\rangle. \quad (15)$$

Because the wave function $|\psi_k^+\rangle$ and $|\psi_k^-\rangle$ are identical at $k = 0$ the contributions from the points \vec{x}_f and \vec{x}_i cancel.

With the help of the Trotter product formula the lefthand side of the equation can be rewritten as a path integral:

$$l.h.s. = \frac{\int_{(\vec{x}_i,0)}^{(\vec{x}_f,\beta)} Dx \exp(-S[x]) o\left(\vec{x}\left(\frac{\beta}{2}\right)\right)}{\int_{(\vec{x}_i,0)}^{(\vec{x}_f,\beta)} Dx \exp(-S[x])} =: \langle o\left(\vec{x}\left(\frac{\beta}{2}\right)\right) \rangle. \quad (16)$$

With equations (6) and (11) one finally finds for the scattering length:

$$a = \frac{1}{32\pi(2m)^{1/2}} \lim_{\beta \rightarrow \infty} \beta^{3/2} \langle o\left(\vec{x}\left(\frac{\beta}{2}\right)\right) \rangle. \quad (17)$$

III. MONTE-CARLO EVALUATION OF THE PATH INTEGRAL

A. Reference potentials

In path integral Monte-Carlo methods a path sampling algorithm is used to generate paths which are distributed according to a (normalized) probability weight

$$P(x) = \frac{\exp(-S[x])}{\int Dx \exp(-S[x])}. \quad (18)$$

The average of an estimator $E(x)$ over the sampled paths approaches the expectation value

$$\lim_{N_s \rightarrow \infty} \frac{1}{N_s} \sum_{l=1}^{N_s} E[x_l] = \int Dx P[x] E[x] =: \langle E \rangle$$

in the limit of an infinite number of samples N_s . In the path integral representations in (7) and (10), the scattering observable is not related to an expectation value of a functional in path space but to the path integral itself. Therefore we still have to construct estimators for scattering observables. Consider the functional

$$E_{\tilde{V}}[x] = \exp \epsilon \sum_{n=0}^{N-1} (V(\vec{x}_n) - \tilde{V}(\vec{x}_n)) = \exp(S_V[x]) \exp(-S_{\tilde{V}}[x]), \quad (19)$$

where \tilde{V} is an arbitrary function. The expectation value of $E_{\tilde{V}}$ is

$$\langle E_{\tilde{V}} \rangle = \frac{\int Dx \exp(-S[x]) E_{\tilde{V}}[x]}{\int Dx \exp(-S[x])} = \frac{\int Dx \exp(-S_0[x] - S_{\tilde{V}}[x])}{\int Dx \exp(-S_0[x] - S_V[x])}. \quad (20)$$

The potential V in the numerator is replaced by the potential \tilde{V} . Therefore from (4) one sees that in the limit of large imaginary time β the expectation value of $E_{\tilde{V}}$ is the ratio of the ground state wave functions of the two potentials [25]:

$$\langle E_{\tilde{V}} \rangle \stackrel{\beta \rightarrow \infty}{=} \frac{\psi_{k=0, \tilde{V}}(\vec{x}_i) \psi_{k=0, \tilde{V}}^\dagger(\vec{x}_f)}{\psi_{k=0, V}(\vec{x}_i) \psi_{k=0, V}^\dagger(\vec{x}_f)} \quad (21)$$

If a solvable reference potential \tilde{V} is chosen which is similar to V the variance of E will be small and the Monte-Carlo algorithm converges rapidly.

Equation (21) can be used to construct an estimator for the ratio of the cross sections of V and \tilde{V} . If the potential V has no zeros we can sample paths which are distributed according to the exponential of a modified action

$$S'[x] = S[x] - \ln V(\vec{x}_f) - \ln V(\vec{x}_i). \quad (22)$$

Unlike the path integral (1) the points \vec{x}_f and \vec{x}_i are no longer fixed but also considered as integration variables. The expectation value of the estimator

$$E'_{\tilde{V}}[x] = \frac{\tilde{V}(\vec{x}_f) \tilde{V}(\vec{x}_i)}{V(\vec{x}_f) V(\vec{x}_i)} E_{\tilde{V}}[x] \quad (23)$$

with paths sampled according to S' is the ratio of the cross sections of V and \tilde{V}

$$\langle E'_{\tilde{V}} \rangle = \frac{\sigma_{\tilde{V}}}{\sigma_V}. \quad (24)$$

If the potential has zeros one can divide the integral over the endpoints \vec{x}_f and \vec{x}_i into parts where the potential does not change sign and perform a simulation for each of these parts. In this case the ratio of cross sections is the sum of these contributions.

An analogous estimator can be constructed for the path integral (9). With the same arguments as before one sees that the expectation value of

$$E(x) = \frac{\exp(-S_{\tilde{V}}[x]) - 1}{\exp(-S_V[x]) - 1} \quad (25)$$

approaches the ratio of the scattering lengths in the limit of large β

$$\langle E \rangle \stackrel{\beta \rightarrow \infty}{=} \frac{a_{\tilde{V}}}{a_V}. \quad (26)$$

B. Langevin simulation

Recently Langevin simulation has been studied as a formal approach to quantum mechanics and as a method for practical calculations (see [26,27] for a review). The basic idea of a Langevin simulation is to solve numerically the stochastic differential equation

$$\frac{\partial}{\partial t} \vec{x}_n(t) = -\frac{\partial}{\partial \vec{x}_n} S[x(t)] + \vec{\eta}_n(t), \quad (27)$$

where $\vec{\eta}_n(t)$ is a Gaussian random variable

$$\langle \eta_{n,i} \rangle = 0 \quad \langle \eta_{n,i}(t) \eta_{m,j}(s) \rangle = 2\delta_{nm} \delta_{ij} \delta(t-s).$$

The time variable t is not the physical time which is represented by the index n here but a simulation time. The Langevin equation (27) describes the dynamics of a whole path which

moves under the influence of a drift force $\vec{\nabla}_n S$ and random fluctuations $\vec{\eta}_n(t)$. One can show that the stochastic process $\vec{x}_n(t)$ is ergodic:

$$\int Dx P[x] E[x] = \lim_{T \rightarrow \infty} \frac{1}{T} \int_0^T dt E[x(t)] \quad (28)$$

with P defined as in (18) and E arbitrary.

The convergence properties of the Langevin equation are related to the Fokker-Planck operator

$$\hat{F} := \sum_n \frac{\partial}{\partial \vec{x}_n} \left(\frac{\partial}{\partial \vec{x}_n} + \frac{\partial S[x]}{\partial \vec{x}_n} \right). \quad (29)$$

which is a differential operator in path space. $P(x)$ is the stationary solution of the Fokker-Planck equation

$$\frac{\partial}{\partial t} \Phi(x, t) = \hat{F} \Phi(x, t), \quad (30)$$

i.e. $\hat{F} P[x] = 0$. The Fokker-Planck equation describes the time evolution of probability distributions of paths. If \hat{F} has a negative discrete spectrum, then $\Phi(x, t)$ in (30) converges to $P[x]$ in the limit $t \rightarrow \infty$ if the initial distribution $\Phi(x, t = 0)$ is not orthogonal on P . In terms of the Langevin equation (27) this means that the distribution function of the stochastic process $\vec{x}_n(t)$ in the limit $t \rightarrow \infty$ is $P[x]$, independent of the initial distribution. The convergence rate, i.e. the typical times T needed in (28), is given by the first nonvanishing eigenvalue of \hat{F} .

For a numerical application one discretizes the Langevin time and simulates the stochastic process

$$\vec{x}_n(t + \Delta t) = \vec{x}_n(t) - \frac{\partial S[x(t)]}{\partial \vec{x}_n} \Delta t + \vec{\Delta} \omega_n(t) \quad (31)$$

$$\langle \Delta \omega_{n,i}(t) \Delta \omega_{m,j}(t) \rangle = \begin{cases} 2\Delta t \delta_{nm} \delta_{ij}, & \text{if } t = s \\ 0, & \text{else} \end{cases} \quad (32)$$

We start from an arbitrary initial path $\vec{x}_n(t = 0)$ and iterate (31) with a sequence of random numbers $\Delta \vec{\omega}_n(t)$. The method (31) corresponds to a simple Euler scheme for the solution of ordinary differential equations. Higher order algorithms have been studied recently [28–30].

C. An example: scattering off a Gaussian potential

After having introduced the formal techniques we will now apply these methods to scattering off a Gaussian potential

$$V(x) = V_0 \exp\left(-\frac{1}{2b^2}x^2\right). \quad (33)$$

As the only relevant parameter of zero energy scattering is $2mV_0b^2$ one can set $b = 1$ and $m = 1$ without loss of generality.

For the method described in section II B, the action S' in equation (22) is inserted into the stochastic differential equation (27). As an initial path of we use

$$\vec{x}_n = \frac{n}{N}(\vec{x}_f - \vec{x}_i) + \vec{x}_i$$

with \vec{x}_f and \vec{x}_i randomly chosen inside the potential. Because of the additional part $\ln V(\vec{x}_i) + \ln V(\vec{x}_f)$ in the action S' (22), the endpoints of the path are subject to a linear drift force in the Langevin simulation which moves them back inside the potential region. Therefore they will not leave the potential under the influence of the stochastic force $\Delta\omega$.

For numerical integration of the path integral defined in II C the action (9) is inserted into the Langevin equation (27). We obtain the stochastic differential equation

$$\frac{\partial}{\partial t}\vec{x}_n(t) = -\frac{\partial S_0[x(t)]}{\partial \vec{x}_n} - \frac{1}{D[x(t)]} \frac{\partial S_V[x(t)]}{\partial \vec{x}_n} + \vec{\eta}_n(t) \quad D[x] := 1 - e^{S_V[x]}. \quad (34)$$

The logarithm in the action disappears, as only the derivative of the action enters into the Langevin equations. For the potential (33), which does not change sign, $D[x]$ is always positive (V repulsive) or negative (V attractive) as $\exp S_V[x]$ is either greater or less than one. For a general potential $D[x]$, can have zeros. In this case the stochastic process defined by (34) is not ergodic. The path space is divided into regions of positive and negative signs of $D[x]$. At the boundaries of this regions the drift force becomes infinite and prevents the stochastic process from moving into another region. From the numerical point of view this means that several simulations with random initial conditions have to be performed to make sure that the whole path space is covered. A more detailed interpretation of the physical

meaning of the term $1/D[x]$ in the stochastic differential equation will be given when we discuss the convergence properties of the algorithms. For the equation (34) we use $\vec{x}_n = 0$ as initial path.

An estimate of the typical times β required in the numerical calculation can be found from the first order Born approximation for the matrix element (7):

$$\sigma \approx \left(4\pi m \int d^3x V(\vec{x})\right)^2 \left(1 - \frac{m \int d^3x \vec{x}^2 V(\vec{x})}{\beta \int d^3x V(\vec{x})}\right) = (2\pi b^2)^3 (4\pi m V_0)^2 \left(1 - \frac{3mb^2}{\beta}\right) \quad (35)$$

For the the choice of parameters $b = 1, m = 1$ the typical physical times will be $\beta \approx 100$

Since analytical estimates of the step size ϵ are in general hard to obtain, we tested discretization errors numerically. For the present work, we used $\epsilon = 0.5$, which resulted in errors less than 5 percent. Typically 25000 warmup steps were taken to equilibrate, followed by 250000 steps of measurement at $\Delta t = 0.04$. This corresponds to a Langevin time of $T = 10000$. The choice of the Langevin parameters is discussed in section IIID where the convergence properties of the algorithm are studied in more detail.

As a reference, we used a square well potential

$$\tilde{V}(r) = \begin{cases} 0 & r > \tilde{R} \\ \tilde{V}_0 & r < \tilde{R} \end{cases}. \quad (36)$$

From equation (35) we see that for not too strong potentials, the cross section and the leading term in $1/\beta$ is given by the zeroth and second moment of the potential. If the parameters \tilde{R} and \tilde{V}_0 are chosen such that these moments are identical for both potentials, we expect that the ratio of cross sections is close to 1 and depends weakly on β . This leads to an initial guess of the parameters of \tilde{V}

$$\tilde{R} = \sqrt{5}b \quad \tilde{V}_0 = 3\sqrt{\frac{\pi}{250}}V_0. \quad (37)$$

We first discuss the β dependence of the result for the potential strengths $V_0 = 0.1, V_0 = -0.3$ and $V_0 = -0.5$. Figure 1 shows the ratio of the cross sections as a function of β . The lines are the analytic result which are obtained by numerically solving the Schroedinger equation for both potentials. The data point correspond to the stochastic result.

The ratio of the cross section is predicted well for $V_0 = 0.1$ and $V_0 = -0.3$ and does not depend on β from $\beta \approx 10$ on. The deviation of the simulation from the exact result is typically below 4 percent. For $V_0 = -0.5$ a stronger β dependence is found and the simulation predicts a result which is approximately 10 percent too large.

Obviously the reference potential (36) which is based on first order Born approximation (35) is not a good model for the scattering potential if V_0 is large. The Gaussian potential has its first bound state at $V_0 \approx -0.67$, whereas the reference potential with the parametrization (37) has its first bound state at $V_0 \approx -0.74$. Therefore the reference potential (36) is too weak if V_0 is close to the bound state value. If we choose the parameters

$$\tilde{R} = 2 \quad \tilde{V}_0 = \frac{V_0 \pi^2}{0.67 \cdot 32} \quad (38)$$

the reference potential also has a bound state at $V_0 = -0.67$. In figure 2 we plot the result for this improved reference potential at $V_0 = -0.5$, with all other parameters unchanged. The result is now almost β independent and deviates by not more than 4 percent from the exact calculation (Note the different scales of fig. 1 and fig. 2). This deviation is the discretization error in ϵ .

From the result in figure 2 one sees clearly the importance of choosing a good reference potential. With the appropriate choice of \tilde{V} the estimator $E_{\tilde{V}}$ does not strongly depend on β and long simulation times can be avoided. In practice one guesses an initial reference potential and improves it gradually until the variance of E is minimal and no β -dependence is observed.

Qualitatively the calculation using the method (10) shows the same β dependence as in figure 1 and 2. In figure 3 the cross section is plotted for the simulation based on (7). One sees that accurate results can be obtained over a wide range of potential strengths and cross sections with the same simulation parameters.

The central question of every Monte-Carlo calculation is whether the equilibrium distribution is sampled correctly and whether enough samples have been chosen to obtain a statistically significant result. The answer to this question can be found by studying the

autocorrelation time of the algorithm. For Fokker-Planck operators with a discrete spectrum one can show [27] that for long times t the correlations of the degrees of freedom decay like

$$\langle x_n(t)x_n(0) \rangle \stackrel{t \rightarrow \infty}{\propto} \exp\left(-\frac{t}{t_{ac}}\right),$$

where the autocorrelation time $t_{ac} = 1/|\lambda|$ is the inverse of the smallest eigenvalue λ of the Fokker-Planck operator. In the next section we will use this concept to give an estimate of the convergence properties of the Langevin simulations. Numerically this question can be answered by studying the dependence of the averaged estimator

$$e(T) = \frac{1}{T} \int_0^T dt E'_V[x(t)] \approx \frac{1}{N_s} \sum_{l=0}^{N_s} E'_V[x(t_l)] \quad (39)$$

on the simulation time T . In figure (4) we plot $e(T)$ for $V_0 = -0.3$ for both methods (7) and (10). One sees strong fluctuations at small T which average out as T increases. From $T = 4000$ on the result is essentially constant.

From this figure one would estimate an autocorrelation time of the order of magnitude of about 1000, i.e. the algorithm produces one independent sample every 25000 paths. This has to be compared with typical values for bound state problems in many body physics of about 10 – 100 paths for one independent sample (see e.g. [11,18] and the references given there). These large autocorrelation times are not a problem of the Langevin algorithm, but a physical property of scattering systems, as will be seen soon.

We now discuss the results for method (17). For this calculation the initial and final point of the path are fixed to $\vec{x}_i = \vec{x}_f = 0$. The stochastic differential equation (27) is used for path sampling. In contrast to the previous methods a reference potential is not needed as equation (17) directly relates the scattering length a to the expectation value of the function $o(r)$. We again plot the result as a function of the simulation time in figure (5). The potential strength is $V_0 = 0.1$. Although the potential is rather weak one needs $T = 100000$, i.e. 2.5×10^6 samples to come close to the analytical result of $a = -0.21$.

The slow convergence of (17) can be understood from the structure of the estimator $o(x)$ and the paths which are generated by the stochastic differential equation. In figure 6 we plot

$o(r)$ and the probability distribution of finding the midpoint of the path at a distance r from the origin. Obviously the midpoint of the paths lies outside the potential most of the times, i.e. at values of r where $o(r)$ is zero. Only few samples contribute to the expectation value $\langle o \rangle$ in (17). For this reason it is not advisable to calculate the scattering length directly with eq. (17). It can be used together with method (7) to determine the sign of the scattering length. The estimator $E'_{\vec{V}}[x]$ in equation (19) yields accurate results for the square of the scattering length and the same paths which are used with $E'_{\vec{V}}[x]$ can be used to measure the sign of a via (17).

D. Estimate of convergence properties

The numerical results presented in the previous section showed that a rather large number of path samples is required in the simulation. Further it was found that the paths are outside the range of the potential most of the time. Both observations are intimately related to the physical properties of scattering systems. They are not an artifact of the algorithm we use.

The reason for both problems is that scattering wave functions are not normalizable. Consider an attractive potential which vanishes at infinity and is strong enough to have a bound ground state at energy E_0 . At $\beta \rightarrow \infty$ the typical spatial extension of the paths is $r \approx 1/\sqrt{2mE_0}$, as the path integral is dominated by the ground state wave function, which decays like $\exp(-\sqrt{2mE_0}r)$. If the potential is too weak to have a bound state the typical extension of the paths diverges as $\beta \rightarrow \infty$, as the zero energy scattering wave function (5) does not vanish at $r \rightarrow \infty$. Therefore one expects that the convergence properties of the Monte-Carlo simulation becomes worse in the limit of large β , which means that the autocorrelation time strongly depends on β .

This can be interpreted intuitively from the properties of the stochastic differential equation (27) with the action S' eq.(22). For a potential V , which is attractive but too weak to have a bound state, the potential drift $\vec{\nabla}_n S_V$ is not strong enough to move the paths back into the range of the potential. If the endpoints of the paths were not fixed inside the range

of the potential by the term $\ln V(\vec{x}_i) + \ln V(\vec{x}_f)$ in S' , they would move to infinity under the influence of the stochastic force $\eta(t)$. The other points of the paths are kept back in the vicinity of the potential by the kinetic energy term S_0 of the action which causes a linear force between neighbouring path points in the stochastic differential equation. For systems with at least one bound state the potential energy is strong enough to keep the paths inside the range of the potential, even if the endpoints are not fixed.

One can give a quantitative result for the typical behaviour of the path points by studying only the kinetic energy part of the action plus the part of the potential which keeps back the endpoints. In this case the stochastic differential equation has the form

$$\frac{\partial}{\partial t} \vec{x}_n = - \sum_{m=0}^N M_{nm} \vec{x}_m(t) + \vec{\eta}_n(t) \quad (40)$$

$$\mathbf{M} = \frac{m}{\epsilon} (2\mathbf{1} - \mathbf{A}), \quad \mathbf{A} := \begin{pmatrix} 1 - \frac{\epsilon}{mb^2} & 1 & 0 & \dots & & & \\ & 1 & 0 & 1 & 0 & \dots & \\ & & 0 & 1 & 0 & 1 & 0 & \dots \\ & & \vdots & & & & & \\ & & & \dots & 0 & 1 & 0 & 1 \\ & & & & \dots & 0 & 1 & 1 - \frac{\epsilon}{mb^2} \end{pmatrix}. \quad (41)$$

This equation describes a set of coupled harmonic oscillators. The eigenvalues of the Fokker-Planck operator are integer multiples of the eigenvalues of $-M$ [27]. Therefore the lowest eigenvalue λ of M is related to the autocorrelation time $t_{ac} = 1/\lambda$.

The eigenvalues of M can be found by numerical diagonalization. In figure 7.1 we show the autocorrelation time at constant $\epsilon = 0.5$ as a function of β for different widths b of the potential which binds the endpoints. t_{ac} diverges like β^2 . For our simulation at $\beta = 100$ we find an autocorrelation time of $t_{ac} \approx 2000$ which agrees with the estimate from plotting $e(T)$ in figure 4.

We also see from figure 7 that the autocorrelation time depends strongly on the width b . In the limit $b \rightarrow \infty$ the endpoints of the paths are no longer fixed in the range of the

potential. In this case the matrix M has one vanishing eigenvalue with the eigenvector $\Phi_{min} \propto (1, 1, \dots, 1)$. This zero mode corresponds to a displacement of the path. The stochastic differential equation is translational invariant in this case. This causes an infinite autocorrelation time as the paths spread over a space with an infinite volume.

Figure (7,2) shows the same calculation but with a small harmonic oscillator potential

$$\frac{1}{2}\epsilon \sum_{n=0}^{N-1} m\omega^2 x_n^2$$

($\omega = 0.1$) added to the action. Independent of the conditions on the endpoints we reach a constant autocorrelation time at large values of β , in agreement with our discussion at the beginning of this section.

Therefore two conditions are necessary for the convergence of the Langevin simulation: One is a boundary condition on the endpoints of the paths and the other is a finite time β . This guarantees a discrete spectrum of the Fokker-Planck operator. The situation is analogous to quantum mechanics on a finite interval. The boundary conditions on the wave function causes the spectrum to be discrete, even for systems which have only scattering states in the continuum limit $L \rightarrow \infty$. The energy gap of a system with a bound state approaches a nonzero value in this limit, for a system with a purely continuous spectrum it vanishes.

A remarkable point in this result is that a connection exists between the spectrum of the Fokker-Planck operator and the Hamiltonian. Although we did not formulate a rigorous proof, it is clear from physical arguments that for actions of the form (2) the Fokker-Planck operator has a continuous spectrum in the limit $\beta \rightarrow \infty$, if the Hamilton operator has a purely continuous spectrum.

Let us briefly discuss the method presented in (10) from the point of view of boundary conditions on the paths. We sum over periodic paths which are not fixed in space. If a path drifts outside the range of the potential, i.e. if S_V in (34) approaches zero, the factor $1/D$ increases the potential drift and moves the path back into the range of the potential. This is true for repulsive and attractive potentials. Therefore the Fokker-Planck operator of the

stochastic differential equation (34) has a discrete spectrum for finite β and the simulation converges.

Numerically we have seen that the convergence properties of the simulations based on (7) and (10) are very similar. The autocorrelation time in both cases is strongly β dependent. The reason for this can be understood by comparing the potential drifts of (34) with the potential drift of e.g. a particle in a harmonic oscillator potential. For the harmonic oscillator every point of the path experiences a linear force moving it back to the origin, whereas in (34) we have an overall factor which only increases the drift if most of the points lie outside the potential. Therefore we still have a diverging autocorrelation time at large β .

One can also give an estimate of the maximum Langevin discretization time Δt from the eigenvalues of M . This quantity is determined by the maximum eigenvalue of M as convergence of the discretized Langevin equation requires $\lambda\Delta t \ll 1$ for all eigenvalues λ . From the Perron-Frobenius theorem for positive matrices [33] it is found that $4m/\epsilon$ is an upper limit for the eigenvalues of M . The step size Δt therefore has to fulfill the condition

$$\Delta t \ll \frac{\epsilon}{4m}. \quad (42)$$

For the parameters used here the upper bound is $\Delta t \ll 0.125$. Numerically strong discretization errors are found close to this value and instabilities of the simulation above the critical value.

IV. MANY-BODY TARGETS

In the previous two sections it has been shown that for potential scattering it is possible to calculate scattering observables at vanishing energy with Monte-Carlo methods. We now give an application to a schematic many-body system in order to show that convergence properties are not fundamentally different for targets with internal degrees of freedom.

Consider a target which consists of a set of A harmonic oscillators with a Hamiltonian

$$H_t = \sum_{a=1}^A \left(\frac{\vec{p}_a^2}{2M} + \frac{1}{2}M\omega^2 \vec{q}_a^2 \right). \quad (43)$$

The projectile interacts with the target via a sum of local two-body potentials

$$V(\vec{x}, \vec{q}_1, \dots, \vec{q}_A) = \sum_{a=1}^A V(\vec{x} - \vec{q}_a).$$

Again the relevant object is the long time limit of the imaginary time propagator. In the absence of a projectile target bound state we find analogous to (4)

$$\langle \vec{x}' \underline{q}' | \exp(-\beta H) | \vec{x} \underline{q} \rangle \stackrel{\beta \rightarrow \infty}{=} \exp(-\beta E_0) \left(\frac{2\pi m}{\beta} \right)^{3/2} \psi_{0,0}(\vec{x}', \underline{q}') \psi_{0,0}(\vec{x}, \underline{q}), \quad (44)$$

where $\psi_{0,0}(\vec{x}, \underline{q})$ is a scattering wave function with the projectile at $k = 0$ and the target in its ground state $|0\rangle$ as incoming wave. E_0 is the ground state energy of the target. We use the notation $\underline{q} = (\vec{q}_1, \dots, \vec{q}_A)$ for the degrees of freedom of the target.

The elastic cross section of the projectile at vanishing energy is:

$$\sigma(E = 0) = \lim_{\beta \rightarrow \infty} (2\pi m \beta)^{1/2} \beta e^{\beta E_0} (2\pi)^3 \langle 0, k = 0 | V e^{-\beta H} V | 0, k = 0 \rangle \quad (45)$$

The matrix element can again be written as a path integral

$$(2\pi)^3 \langle 0, k = 0 | V e^{-\beta H} V | 0, k = 0 \rangle = \sum_{a', a=1}^A \int d^{3A} q_i d^{3A} q_f d^3 x_i d^3 x_f V(\vec{x}_i - \vec{q}_{a,i}) \Phi_0(\underline{q}_i) V(\vec{x}_f - \vec{q}_{a',f}) \Phi_0(\underline{q}_f) \times \int_{\vec{x}_i \underline{q}_i}^{\vec{x}_f \underline{q}_f} Dx Dq \exp(-S[x, q]) \quad . \quad (46)$$

$\Phi_0(\underline{q}) = \langle \underline{q} | 0 \rangle$ is the target ground state wave function.

As the propagator of the harmonic oscillator is known in closed form one can use an improved Trotter-product formula and insert for one time step

$$\langle \vec{x}' \underline{q}' | \exp(-\epsilon H) | \vec{x} \underline{q} \rangle \approx G_0^{HO}(\underline{q}', \underline{q} | \epsilon) \left(\frac{m}{2\pi\epsilon} \right)^{3/2} \exp \left(-\left(\frac{m}{2\epsilon} (\vec{x}' - \vec{x})^2 + \epsilon \sum_{a=1}^A V(\vec{x} - \vec{q}_a) \right) \right) \quad (47)$$

with the imaginary time propagator

$$G_0^{HO}(\underline{q}', \underline{q} | \epsilon) = \left(\frac{M\omega}{2\pi \sinh \omega\epsilon} \right)^{3/2} \exp \left(-\frac{M\omega}{2 \sinh \omega\epsilon} ((\underline{q}'^2 + \underline{q}^2) \cosh \omega\epsilon - 2\underline{q}'\underline{q}) \right) \quad (48)$$

for the harmonic oscillator. Using this path integral means that we have no discretization error in the propagation of the target alone, as we summed up the full dynamics of the target

already. Unfortunately there are, to our knowledge, no closed expressions for propagators of scattering systems in three dimensions. If an exact expression for the dynamics of the projectile could be found, only the interplay of the projectile and target degrees of freedom would determine the size of the time step ϵ . As the autocorrelation time critically depends on the number of time steps for scattering systems, improved short time propagators [31,32] could be particularly helpful for practical applications.

The treatment of the endpoints of the paths can be performed in the same way as for potential scattering by simulating the modified action

$$S'[x, q] = S[x, q] - \ln \Phi_0(\underline{q}_i) - \ln \Phi_0(\underline{q}_f) - \ln \sum_a V(\vec{x}_i - \vec{q}_{a,i}) - \ln \sum_a V(\vec{x}_i - \vec{q}_{a,f}) \quad (49)$$

For a many-body system the integral over the endpoints of the paths is high dimensional and can only be handled by stochastic integration.

In equation (49) the logarithm of the ground state wave function is added to the action. For the problem discussed here this is a harmonic oscillator wave function which is analytically known. At the end of this section we will briefly comment on how this formula can be generalized to applications where the ground state wave function of the target is not known.

As an estimator a functional analogous to (19) can be used [8]

$$E[x, q] = \exp \epsilon \sum_{n=0}^{N-1} \left(\sum_{a=1}^A V(\vec{x}_n - \vec{q}_{n,a}) - V_{eff}(\vec{x}_n) \right). \quad (50)$$

Here the coupling of projectile and target degrees of freedom is replaced by an effective potential V_{eff} which only contains the projectile degrees of freedom. Unlike the traditional approach to nuclear multiple scattering [2–4] where the many body problem is approximated by an effective optical potential, no approximations are made here. The Monte-Carlo method yields an exact result and compares it with the effective potential.

With the same arguments as for potential scattering one can show that measuring the estimator (50) with paths sampled with the modified action (49) yields in the limit of large imaginary time β

$$\langle E \rangle \stackrel{\beta \rightarrow \infty}{=} \frac{\langle k=0 | V_g | \psi_{k=0}^{V_{eff}} \rangle \langle \psi_{k=0}^{V_{eff}} | V_g | k=0 \rangle}{\langle 0, k=0 | V | \psi_{0,0} \rangle \langle \psi_{0,0} | V | 0, k=0 \rangle}, \quad (51)$$

with the folded potential

$$V_g(\vec{x}) = \int d^3q |\Phi_0(\underline{q})|^2 \sum_{a=1}^A V(\vec{x} - \vec{q}_a). \quad (52)$$

The quantity in the denominator is the cross section of the full many body problem whereas the numerator can be found as the solution of a potential scattering problem. If one uses the corrected estimator

$$E'[x, q] = E[x, q] \frac{V_{eff}(\vec{x}_f) V_{eff}(\vec{x}_i)}{V_g(\vec{x}_f) V_g(\vec{x}_i)} \quad (53)$$

one again finds that the expectation value of E' is the ratio of the cross sections

$$\langle E' \rangle \stackrel{\beta \rightarrow \infty}{=} \frac{\sigma_{V_{eff}}}{\sigma}.$$

There is one major difference as compared to the potential scattering calculation. One can always find an estimator $E_{\tilde{V}}$ with a vanishing variance for potential scattering by setting $\tilde{V} = V$. In other words: we know that there are model potentials which are arbitrarily close to the potential which we want to study. This is not true for the estimator (50), because correlations of target and projectile degrees of freedom can not be modeled with a one-body potential. The variance of E in the simulation will show whether this is possible or not.

As we are dealing in the following with a system of distinguishable identical particles we can further simplify the treatment of the endpoint by decomposing the sum (45) into a indirect contribution σ_i , where the projectile path begins and ends at different nucleons, and an indirect contribution σ_d , where the projectile path begins and ends at the same nucleon

$$\begin{aligned} \sigma(E=0) &= A\sigma_d + A(A-1)\sigma_i \\ \sigma_d &= \lim_{\beta \rightarrow \infty} (2\pi m\beta)^{1/2} \beta e^{\beta E_0} \langle 0, k=0 | V(\vec{x} - \vec{q}_1) e^{-\beta H} V(\vec{x} - \vec{q}_1) | 0, k=0 \rangle \\ \sigma_i &= \lim_{\beta \rightarrow \infty} (2\pi m\beta)^{1/2} \beta e^{\beta E_0} \langle 0, k=0 | V(\vec{x} - \vec{q}_1) e^{-\beta H} V(\vec{x} - \vec{q}_2) | 0, k=0 \rangle. \end{aligned}$$

The advantage of this procedure as compared to (49) is that one has already isolated the factors A and $A(A-1)$ correctly. If one simply inserts (49) into the stochastic differential equation and starts the calculation with a initial path which begins and ends at the same

nucleon it might take a long time T until the simulation reached a path which begins and ends at different nucleons. After splitting the path integral into the direct and indirect contribution one can perform two independent simulations with actions

$$S_d[x, q] = S[x, q] - \ln \Phi_0(\underline{q}) - \ln \Phi_0(\underline{q}') - \ln V(\vec{x} - \vec{q}_1) - \ln V(\vec{x}' - \vec{q}'_1)$$

$$S_i[x, q] = S[x, q] - \ln \Phi_0(\underline{q}) - \ln \Phi_0(\underline{q}') - \ln V(\vec{x} - \vec{q}_1) - \ln V(\vec{x}' - \vec{q}'_2).$$

We finally get for the cross section

$$\frac{\sigma}{\sigma_{V_{eff}}} \stackrel{\beta \rightarrow \infty}{=} A \frac{1}{\langle E' \rangle_d} + A(A-1) \frac{1}{\langle E' \rangle_i}. \quad (54)$$

One could also specify two independent reference potentials V_{eff}^i and V_{eff}^d to define a direct and indirect observable.

In the following this formalism is applied to scattering of a system of four independent particles in a harmonic oscillator potential as a simple model for a ${}^4\text{He}$ nucleus. We focus here on the convergence properties of the algorithm in the regime of strong multiple scattering effect. As interaction between target and projectile the potential (33) with $b = 0.6$ fm is used. The mass of projectile and target are set to $m = M = 1$ GeV ≈ 5 fm $^{-1}$. The oscillator frequency is $\omega = 0.075$ fm $^{-1}$ which corresponds to a mean square radius of the nucleus of 4 fm 2 and an energy gap of $\Delta E = E_1 - E_0 = 15$ MeV.

For our calculation we use the folded potential (52) as an effective potential for the direct and indirect observable. If only the ground state of the target contributes as intermediate state the folded potential gives the correct cross section. Therefore the deviation of the ratio of the cross sections (54) from one is related to the contribution of excited states of the target in the Born series.

The convergence properties of the simulation can again be studied by plotting the average of E' (53) as a function of the simulation time T analogous to eq.(39). In figure 8 the predicted ratio of cross sections for one and four nucleons at $\beta = 80$ MeV $^{-1}$ is shown. The same discretization was chosen as for potential scattering.

As expected the result is close to one for the weakly attractive potential $V_0 = -10$ MeV and does not fluctuate strongly. The ground state of the target dominates the Born series

and the folded potential is a good model. The projectile-nucleus scattering length predicted by the Monte-Carlo calculation is $a_4 \approx 0.75$ fm whereas the scattering length off one bound nucleon is $a_1 \approx 0.15$ fm. This shows that essentially only single scattering occurs as $a_4 \approx 4a_1$.

For the strongly attractive potential $V_0 = -40$ MeV the situation is different. The projectile-nucleus scattering length is predicted to be $a_4 \approx 240$ fm and the scattering length of a single bound nucleon $a_1 \approx 1$ fm. Therefore for this choice of the potential multiple scattering effects play a dominant role and the folded potential is no longer a good model as excited states of the target become important as intermediate states.

The statistical fluctuation in this case are larger than for the weak potential $V_0 = -10$ MeV. Figure 8 shows, however, that even for $V_0 = -40$ MeV the simulation has a stable equilibrium value at $T = 10000$ fm². This demonstrates that the method is well suited for calculations where multiple scattering effects dominate.

No qualitative differences are observed in the fluctuations for one and four nucleons. This indicates that also simulations with much more than four nucleons are possible, as the computational effort scales like the number of target particles.

Finally we will briefly comment on how the treatment of the endpoints has to be modified if the ground state wave function of the target is not known in a closed form. In this case one can use that the Hamiltonian of the target H_t projects a trial state $|\tilde{0}\rangle$ on the true ground state

$$e^{-\beta_1 H_t} |\tilde{0}\rangle \stackrel{\beta_1 \rightarrow \infty}{\underset{\approx}{\longrightarrow}} e^{-\beta_1 E_0} |0\rangle.$$

We can therefore modify equation (45) by using the expression

$$\sigma(E=0) = \lim_{\beta \rightarrow \infty} (2\pi)^3 (2\pi m \beta)^{1/2} \beta e^{(\beta+2\beta_1)E_0} \langle \tilde{0} | e^{-\beta_1 H_t} \langle k=0 | V e^{-\beta H} V | k=0 \rangle e^{-\beta_1 H_t} | \tilde{0} \rangle. \quad (55)$$

The time β_1 has to be chosen large on the scale of the target dynamics. The path integral which follows from (55) contains projectile paths of length β and target paths of length $\beta + 2\beta_1$. In the simulation we add the logarithm of the trial wave function to the action of

the target degrees of freedom in order to fix the endpoints. The folded potential can also be found numerically from

$$V_g(\vec{x}) \stackrel{\beta_1 \rightarrow \infty}{=} \frac{\langle \tilde{0} | \exp(-\beta_1 H_t) V(x, \underline{q}) \exp(-\beta_1 H_t) | \tilde{0} \rangle}{\langle \tilde{0} | \exp(-2\beta_1 H_t) | \tilde{0} \rangle}.$$

Therefore more complicated Hamiltonians for the target than (43) cause no fundamental complications.

V. CONCLUSION

The basic goal of this work was to show that Monte-Carlo methods can be applied successfully to scattering problems in cases where the target has internal degrees of freedom. One possible application is nuclear multiple scattering, but the methods developed here should also be useful in atomic and molecular physics.

We showed for potential scattering and scattering of a schematic ^4He nucleus that despite the continuous spectrum of the systems one can perform Monte-Carlo calculations, if one uses the concept of a reference potential to reduce statistical fluctuations. For many-body systems a one-body reference potential is only a first step in constructing optimal observables. It would be useful to find solvable schematic models which take into account the coupling of projectile and target degrees of freedom.

For a phenomenological application of our results a number of questions have to be answered: important candidates for calculations in nuclear scattering are antiprotons and K^- mesons where the scattering lengths are comparable or larger than typical internuclear distances [1–3]. In both systems annihilation of the projectile plays an important role. This is modeled frequently by complex potentials [34], which are not suitable for Monte-Carlo calculations. In order to study these problems one has to find models for annihilation which can be implemented in a Monte-Carlo calculation. Another open question is how to deal with the spin of nucleons. It is well known that antisymmetrization is very important for nucleons as projectiles [35]. A related problem is the implementation of spin-orbit interactions. A

problem of all Monte-Carlo algorithms is, that they only converge to the ground state of the physical system. Scattering observables can therefore only be calculated in absence of a projectile bound state.

The main advantage of the methods we presented is that one can find numerical solutions for a class of many-body problems without approximations on the target dynamics. Questions like in-medium effect in nuclear scattering and the reduction to effective potentials can be investigated by purely microscopic calculations.

A further improvement of the methods seems to be possible in several ways: introducing improved short time propagators (see e.g. [31,32]) will increase the convergence rate of the simulations. So far there are very few results on how improved propagator can be constructed for scattering systems. One of the great achievements of multiple scattering theory is that it is formally possible to separate elementary processes on one nucleon from the multiple scattering dynamics [36,37]. A similar formal structure has not yet been developed in a path integral framework.

Another question is whether it is possible to design path sampling algorithms which are optimized for scattering problems. As scattering paths move outside the range of the potential most of the time it might be possible to find algorithms which use the fact that the functional form of the solution in the outside space is known exactly. Langevin simulation seems to be a promising method of developing new algorithms because the convergence properties of the simulation can be studied in terms of the spectrum of the Fokker-Planck operator. For numerical applications, however, hybrid algorithms [38,39] which are based on stochastic and deterministic dynamics in path space may be more useful. The applicability of these methods to scattering problems is currently studied.

ACKNOWLEDGEMENTS

We would like to thank Prof. F. Lenz who initiated this work and contributed many valuable ideas. Further we thank Prof. J. Koch and Prof. M. Thies for many discussions

and T. Kraus for assistance with numerical algorithms for differential equations.

APPENDIX A: PROOF OF EQUATION (12)

Equation (12) can be derived from the scale transformation properties of the Lippmann-Schwinger equation [24]. The operator

$$U = e^{(i\vec{x}\vec{p} + \frac{3}{2}) \ln \lambda} \quad (\text{A1})$$

generates scale transformations

$$U\vec{x}U^\dagger = \lambda\vec{x} \quad U\vec{p}U^\dagger = \frac{1}{\lambda}\vec{p}.$$

One can define a rescaled T -matrix and momentum eigenstates:

$$\langle \vec{p}_i | T(E) | \vec{p}_f \rangle = \langle \lambda \vec{p}_i | T_\lambda(E) | \lambda \vec{p}_f \rangle \quad (\text{A2})$$

$$T_\lambda(E) = UT(E)U^\dagger \quad |\lambda \vec{p}\rangle = U|\vec{p}\rangle$$

As the matrix element in equation (A2) does not depend on λ one finds:

$$\frac{d}{d\lambda} \langle \lambda \vec{p}_i | T_\lambda(E) | \lambda \vec{p}_f \rangle = 0 \quad (\text{A3})$$

From this equation one gets after setting $\lambda = 1$

$$T' = \frac{1}{1 - VG_0} (2V(\vec{x}) + \vec{x}\vec{\nabla}V(\vec{x})) \frac{1}{1 - G_0V} - 2T + 2E \frac{d}{dE} T. \quad (\text{A4})$$

with the definition $T' = \left. \frac{d}{d\lambda} T_\lambda \right|_{\lambda=1}$. For this equation we used that T is the solution of the operator equation

$$T(E) = V + V \frac{1}{E - H_0 + i\epsilon} T(E).$$

Furthermore:

$$2E \frac{d}{dE} T(E) = p \frac{d}{dp} T(E(p)).$$

In order to prove (12) we have to write the derivative with respect to λ of the momentum eigenstates as derivatives with respect to p . It is easy to show that

$$\left. \frac{d}{d\lambda} \langle \lambda \vec{p}_i | T(E) | \lambda \vec{p}_f \rangle \right|_{\lambda=1} = p \frac{d}{dp} \langle \vec{p}_i | T(E) | \vec{p}_f \rangle - 3 \langle \vec{p}_i | T_\lambda(E) | \vec{p}_f \rangle, \quad (\text{A5})$$

where the operator d/dp only acts on the arguments of the momentum eigenstates. From the equations (A3), (A4), (A5) and the definition of the wave functions

$$|\psi_k^+\rangle = \frac{1}{1 - G_0 V} |\vec{k}\rangle \quad \langle \psi_k^-| = \langle \vec{k}| \frac{1}{1 - V G_0}$$

equation (12) follows immediately.

APPENDIX B: TECHNICAL REMARKS

All Monte-Carlo simulation in this work were done on an HP9000/720 workstation. A simulation at $\beta = 100$ and $\epsilon = 0.5$ for potential scattering with 250000 path samples requires approximately 40 CPU-minutes for method (7). The code is written in standard FORTRAN 77. Method (10) needs about the same amount of time. As the convergence properties of the many body problem which we studied are comparable to potential scattering, the computation time scaled with the number of degrees of freedom. For the ${}^4\text{He}$ calculation 5 hours of CPU time were needed for one simulation run. Tests with improved random number generators and higher order Langevin algorithms showed that an increase of speed by a factor of 5 should be possible but we did not study this systematically.

REFERENCES

- [1] C. B. Dover, “Antinucleon-Nucleus Interactions”, *in* “Physics at LEAR with Low Energy Antiprotons”, Proceedings of the fourth LEAR Workshop, Harwood Academic Publishers, Chur, 1988.
- [2] J. M. Eisenberg und D. S. Koltun, “Theory of Meson Interactions with Nuclei”, ch. 4 and 5, John Wiley, New York, 1980.
- [3] J. Hüfner, Phys. Rep. **21** (1975), 1.
- [4] L. L. Foldy und J. D. Walecka, Ann. Phys. (N.Y.) **54** (1969), 447.
- [5] C. J. Batty, *in* “Proceedings of the 12 th Int.Conf. on Few Body Problems in Physics”, Vancouver, 1989.
- [6] E. Friedman, A. Gal und C. J. Batty, Phys. Lett. **B 308** (1993), 6.
- [7] F. Lenz and D. Stoll, *in* “Computational Nuclear Physics 2” (K. Langanke, J. A. Maruhn and S. E. Koonin Eds.), Springer, New York, 1993.
- [8] S. Lenz and D. Stoll, Z. Phys. **A 351** (1995) 19.
- [9] J. W. Negele und H. Orland, “Quantum Many-Particle Systems”, Addison Wesley, Reading, Massachusettes, 1988.
- [10] M. H. Kalos und P. A. Whitlock, “Monte Carlo Methods Vol. 1: Basics”, John Wiley, New York, 1986.
- [11] M. Creutz, “Quarks, Gluons and Lattices”, Cambridge University Press, Cambridge, 1985.
- [12] J. A. Carlson, Nucl. Phys. **A 508** (1990), 141c.
- [13] G. H. Lang, C. W. Johnson, S. E. Koonin and W. E. Ormand, Phys. Rev. **C 48** (1993), 1518.

- [14] M. H. Kalos, D. Levesque and L. Verlet, *Phys. Rev. A* **9** (1974) 2178.
- [15] P. A. Whitlock, D. M. Cheperley, G. V. Chester and M. H. Kalos, *Phys. Rev.* **B 19** (1979), 5598.
- [16] M. H. Kalos, M. A. Lee, P. A. Whitlock and G. V. Chester, *Phys. Rev.* **B 24** (1981), 115.
- [17] U. Helmbercht and J. G. Zabolitzky, “Droplets of ^4He Atoms”, *in* “Monte-Carlo Methods in Quantum Problems” (M. H. Kalos Ed.), Reidel, Dodrecht, 1982.
- [18] E. Y. Loh and J. E. Gubernatis, “Stable Numerical Simulations of Models of Interacting Electrons in Condensed-Matter Physics”, *in* “Electronic Phase Transitions” (W. Hanke and Yu. V. Kopayev Eds.), Elsevier Science Publishers B.V., 1992.
- [19] W. von der Linden, *Phys. Rep.* **220** (1992), 53.
- [20] R. P. Feynman and A. R. Hibbs, “Quantum Mechanics and Path Integrals”, McGraw-Hill, New York, 1965.
- [21] D. Gelman und L. Spruch, *J. Math. Phys.* **10** (1969), 2240.
- [22] R. G. Newton, “Scattering Theory of Waves and Particles”, ch. 11, Springer Verlag, New York, 1982.
- [23] R. Dashen, S. Ma and H. Bernstein, *Phys. Rev.* **187**, (1969) 345.
- [24] F. Lenz, lecture on “Monte-Carlo Methods for Scattering Problems”, Erlangen, 1993.
- [25] S. Lenz, “Stochastic Methods for Quantum Scattering”, conference contribution to the “6. Joint EPS-APS International Conference on Physics Computing”, Lugano, 1994, preprint nuc-th/9402030.
- [26] G. Parisi and Wu Yongshi, *Sci. Sin.* **24** (1981) 483.
- [27] M. Namiki, “Stochastic Quantization”, Springer Verlag, Berlin, Heidelberg, 1992.

- [28] A. S. Kronfeld, Progress of Theoretical Physics Supplement **111** (1993), 293.
- [29] A. Greiner, W. Strittmatter and J. Honerkamp, J. Stat. Phys. **51** (1988), 95.
- [30] P. E. Kloeden and E. Platen, J. Stat. Phys. **66** (1992), 283.
- [31] N. Makri und W. H. Miller, J. Chem. Phys. **90** (1989), 904.
- [32] I. Bender, D. Gormes und U. Marquard, Nucl. Phys. **B 346** (1990), 593.
- [33] A. Graham, “Nonnegative Matrices and Applicable Topics in Linear Algebra”, p.114, Ellis Horwood Ltd., Chichester, 1987.
- [34] M. Kohno and W. Weise, Nucl. Phys. **A454** (1986), 429.
- [35] A. K. Kerman, M. McManus, R. M. Thaler, Ann. Phys. (N.Y.) **8** (1959), 551.
- [36] L. S. Rodberg und R. M. Thaler, “Introduction to The Quantum Theory of Scattering”, ch. 12, Academic Press, New York, 1967.
- [37] M. L. Goldberger and K. M. Watson, “Collision Theory”, ch. 11, John Wiley, New York, 1964.
- [38] S. Duane, A. D. Kennedy, J. P. Pendleton, D. Roweth, Phys. Lett. **B 195** (1987), 216.
- [39] P. B. Mackenzie, Phys. Lett. **B 226** (1989), 369.

FIGURES

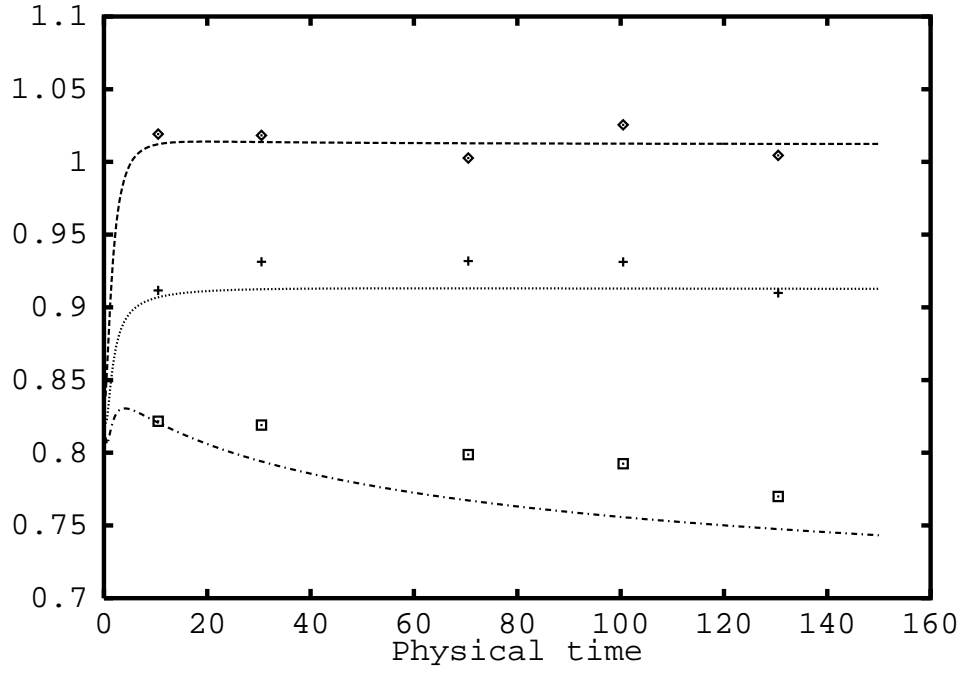


FIG. 1. Ratio of the cross sections of the square well potential an the Gaussian potential as a function of the physical time β . The line is the solution of the Schroedinger equation, data points are the results of the Langevin simulation. $V_0 = 0.1$ (\diamond), $V_0 = -0.3$ (+) and $V_0 = -0.5$ (\square) with the reference potential (36,37).

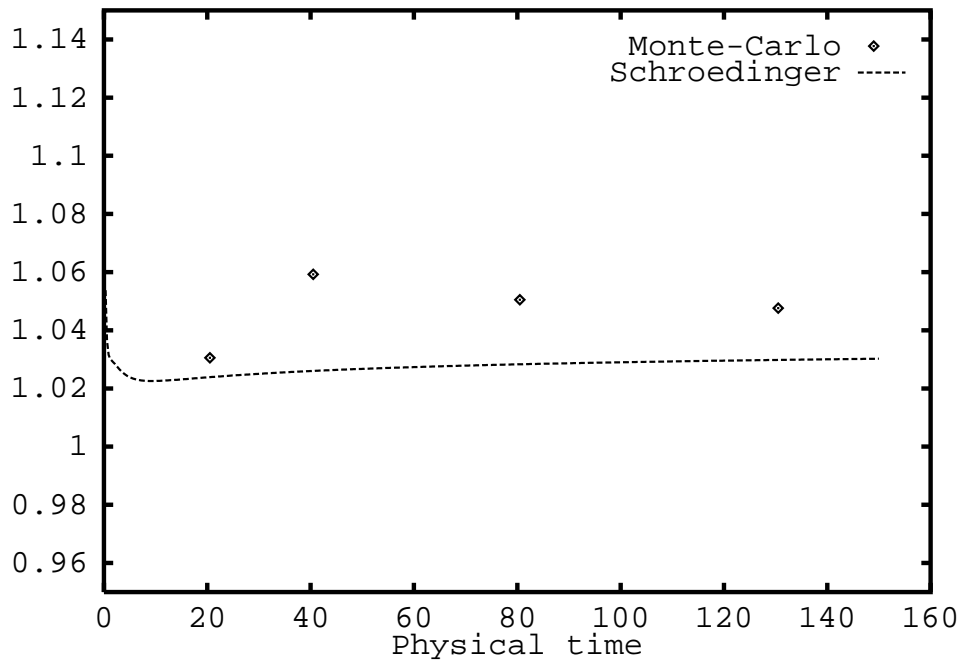


FIG. 2. The same calculation as in figure 1 using a modified reference potential (38) for $V_0 = -0.5$. (\diamond): Monte-Carlo result, Line: Schrodinger equation. Note the different scale!

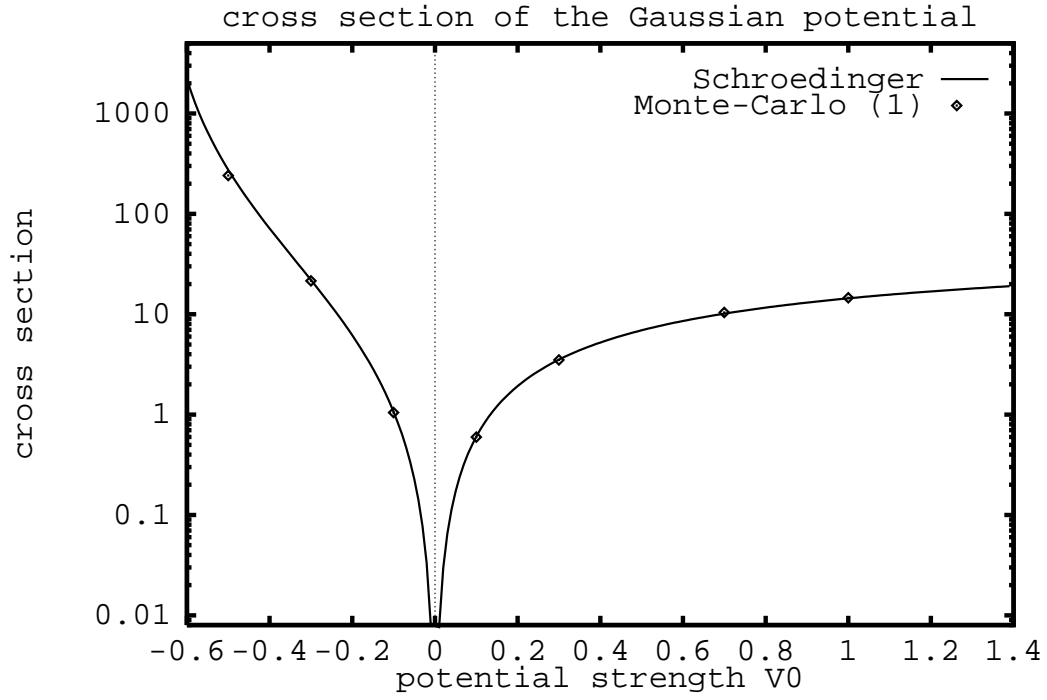


FIG. 3. The cross section of the Gaussian potential as a function of V_0 . The line is the result of the Schrodinger equation, data points are the Monte-Carlo simulation (7).

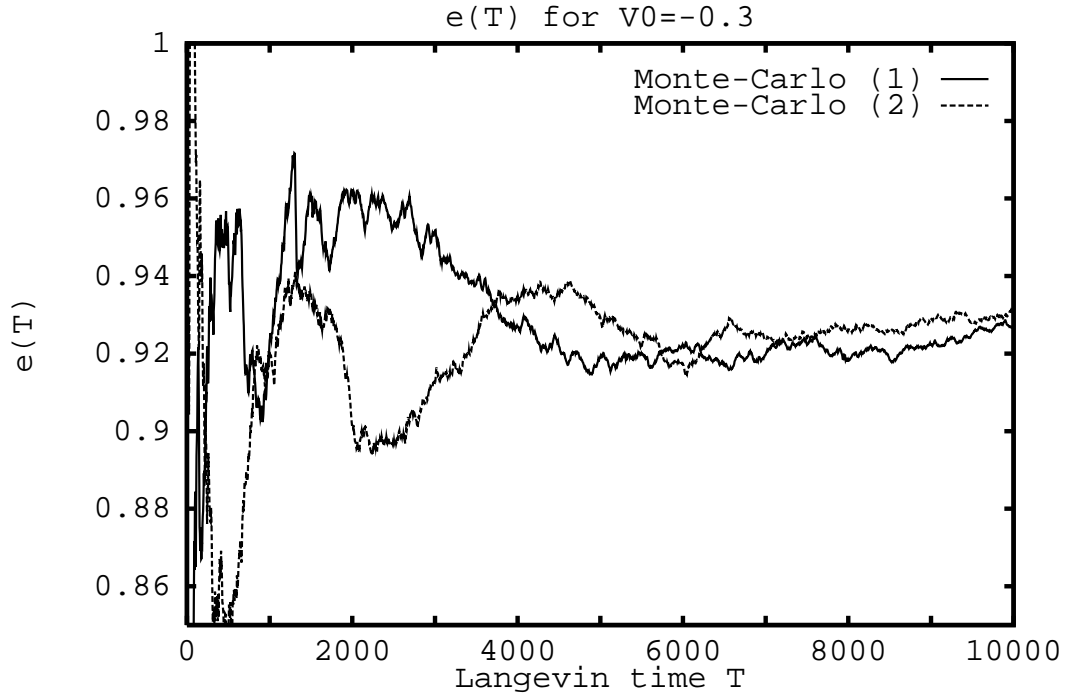


FIG. 4. The prediction of the ratio of the cross sections of the Gaussian potential and the reference potential as a function of the simulation time T at $V_0 = -0.3$. Monte-Carlo (1) uses (7), Monte-Carlo (2) uses (10).

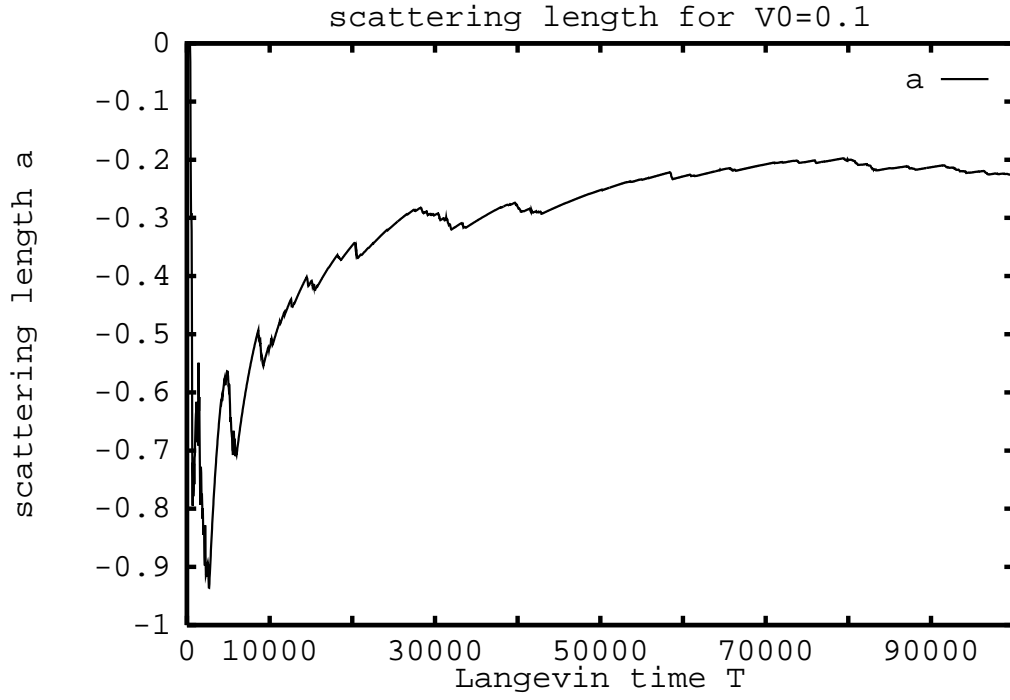


FIG. 5. The scattering length a for $V_0 = 0.1$ as a function of the simulation time T at $\beta = 100$.
the exact value is $a = -0.21$.

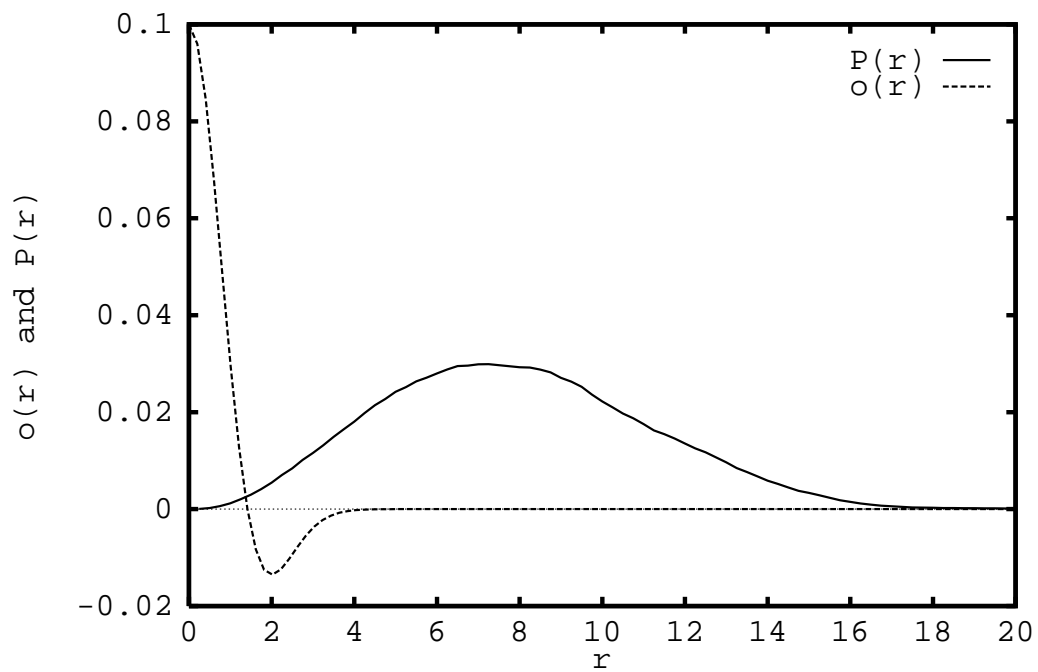


FIG. 6. Probability distribution of path midpoints for $V_0 = 0.1$ and $o(r)$ as a function of the distance r .

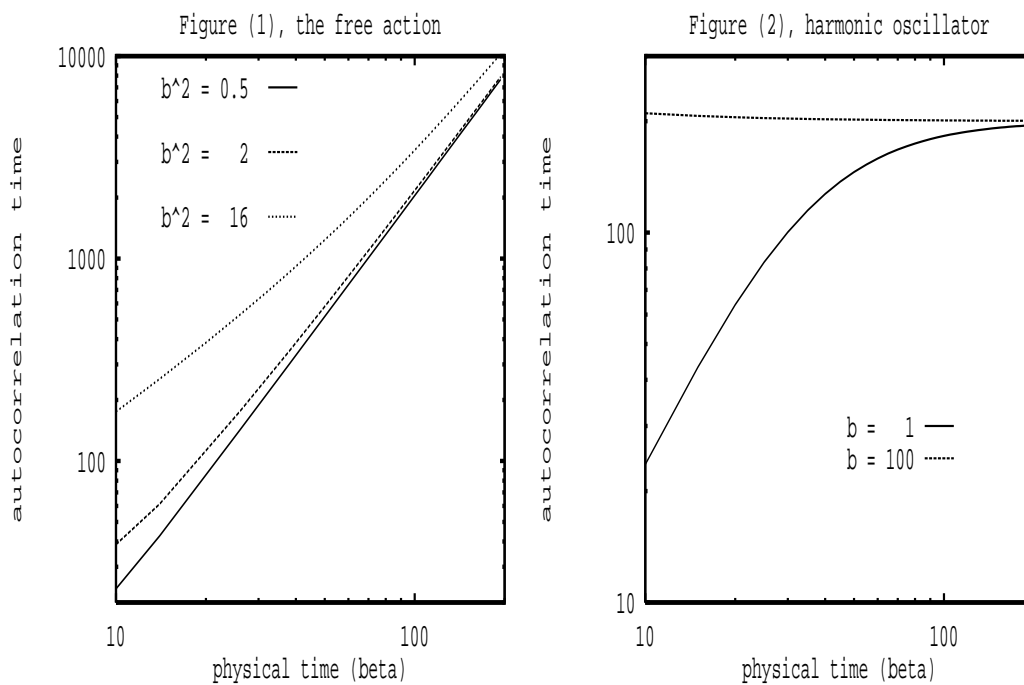


FIG. 7. The autocorrelation time t_{ac} for the free action. Figure (1): t_{ac} as a function of the physical time β for $\epsilon = 0.5$. Figure (2): the free action plus a weak harmonic oscillator potential ($\omega = 0.1$).

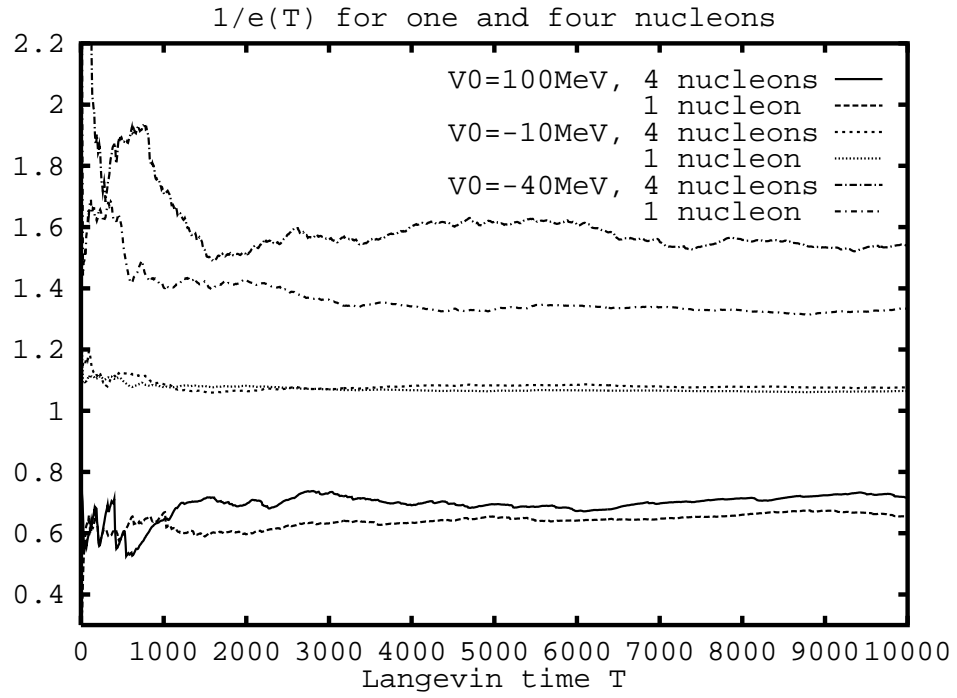


FIG. 8. The ratio of cross sections of the full problem and the effective potential $1/e(T)$ as a function of the Langevin time T for nucleon and for four nucleons.